

Self-assembly of iron nanoclusters on the $\text{Fe}_3\text{O}_4(111)$ superstructured surface

N. Berdunov, G. Mariotto, S. Murphy, K. Balakrishnan, and I. V. Shvets

SFI Laboratories, Department of Physics, Trinity College, Dublin, Ireland

(Received 10 May 2004; revised manuscript received 6 October 2004; published 16 March 2005)

We report on the self-organized growth of a regular array of Fe nanoclusters on a nanopatterned magnetite surface. Under oxidizing preparation conditions, the (111) surface of magnetite exhibits a regular superstructure with three-fold symmetry and a 42 Å periodicity. This superstructure represents an oxygen-terminated (111) surface, which is reconstructed to form a periodically strained surface. A Fe film of 0.5 Å thickness was deposited on this surface at room temperature. Fe nanoclusters are formed on top of the surface superstructure creating a regular array with the periodicity of the superstructure. We demonstrate that at higher coverage Fe growth switches from two- to three-dimensional mode. In the areas of the surface where the strain pattern is not formed, random nucleation of Fe was observed.

DOI: 10.1103/PhysRevB.71.113406

PACS number(s): 68.47.Gh, 68.47.Jn, 68.35.Bs, 68.37.Ef

I. INTRODUCTION

Studies of the self-assembly of nanoclusters into ordered arrays are of great fundamental and technological importance. Nanostructures exhibit many novel physical and chemical properties, which are essential for a fundamental understanding of condensed matter. Moreover, self-assembled nanostructures have enormous potential for technological applications. Increased constraints in lithography technologies have stimulated interest in radically alternative approaches to fabricating structures at the nanometer scale to ensure a continuous progress toward the downsizing of electronics devices. In this respect, self-assembly is a highly promising avenue. For example, it is known that quantum dots can be formed on semiconductor substrates as a result of the strain induced during the heteroepitaxial growth of lattice-mismatched materials. By controlling the dimension and density of these quantum dot arrays, materials with novel optical and electronic properties can be engineered.¹⁻³ Self-assembly of magnetic nanostructures is also a field of great interest. For example, magnetic media with enhanced in-plane magnetoresistance have been constructed utilizing self-assembled nanogranular magnetic films.^{4,5}

The growth of metal nanostructures on oxide substrates is an area of particular importance, since nanostructures grown on metal substrates are not suitable for many applications involving electron transport measurements. This area of research is still mostly unexplored. Previous studies of metal growth on Al_2O_3 and TiO_2 substrates^{6,7} suggest a complex behavior of metal films and small particles on oxide support. Only recently has the wetting behavior of palladium grown on a thin FeO film been demonstrated⁸ and regular arrays of metal nanoclusters were successfully formed on a nanopatterned alumina substrate.⁹

In this paper, we demonstrate that a well-ordered array of Fe nanoclusters can be grown on the patterned surface of $\text{Fe}_3\text{O}_4(111)$. Importantly, the observed nanoclusters were grown and analyzed at room temperature.

II. EXPERIMENTAL RESULTS

The experiments were performed in an ultrahigh vacuum (UHV) at room temperature, using scanning tunneling mi-

croscopy (STM), low-energy electron diffraction (LEED), and Auger electron spectroscopy. A synthetic single crystal of $\text{Fe}_3\text{O}_4(111)$ was used in these experiments. The details of the sample preparation are described elsewhere,¹⁰ but in brief, the preparation consisted of annealing the sample in an oxygen atmosphere of 10^{-6} Torr at a temperature of about 1000 K and then cooling it down at this oxygen pressure.

As reported in our recent publication,¹⁰ under oxidizing preparation conditions, the (111) surface of magnetite reconstructs into a well-ordered superstructure with a periodicity of 42 Å and threefold symmetry, which could be clearly identified by LEED. A STM image of this superstructure is shown in Fig. 1. Three distinct areas, marked as Areas I, II, and III, can be identified. The atomic symmetry of all three areas is identical but they differ in their interatomic periodicity. Areas II and III have a 2.8 Å average periodicity, while the periodicity of Area I is about 3.1 Å. This surface corresponds to the oxygen termination of the bulk magnetite

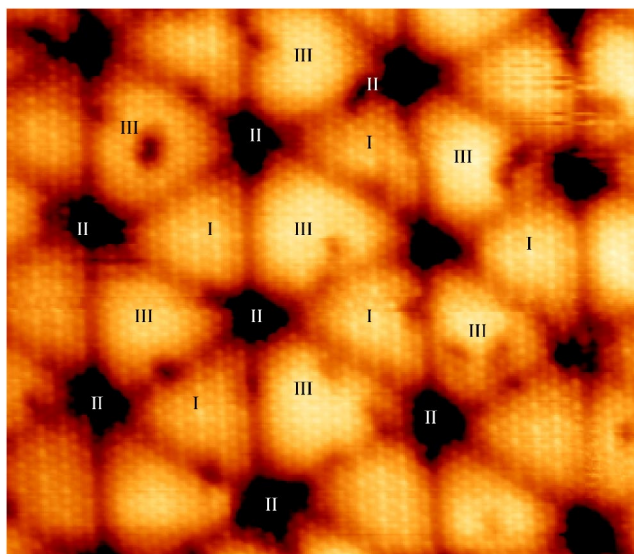


FIG. 1. (1500 Å × 1300 Å) STM image of the surface superstructure. Three distinct areas are marked as I, II, and III. The periodicity of the superstructure is 42 Å.

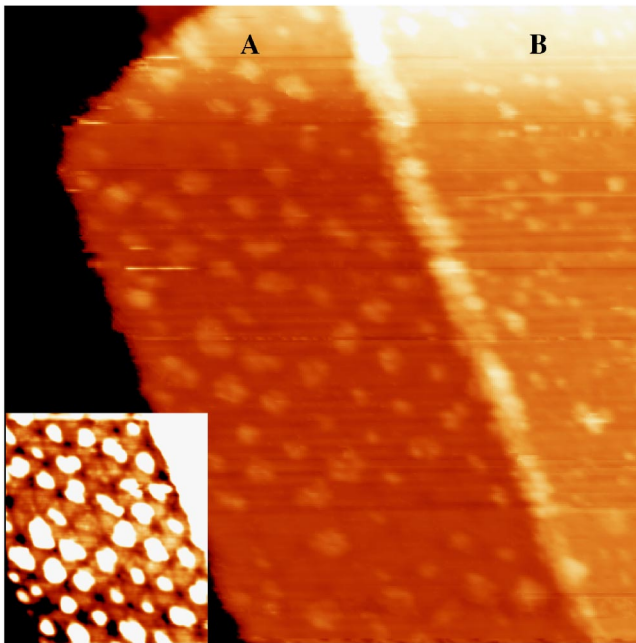
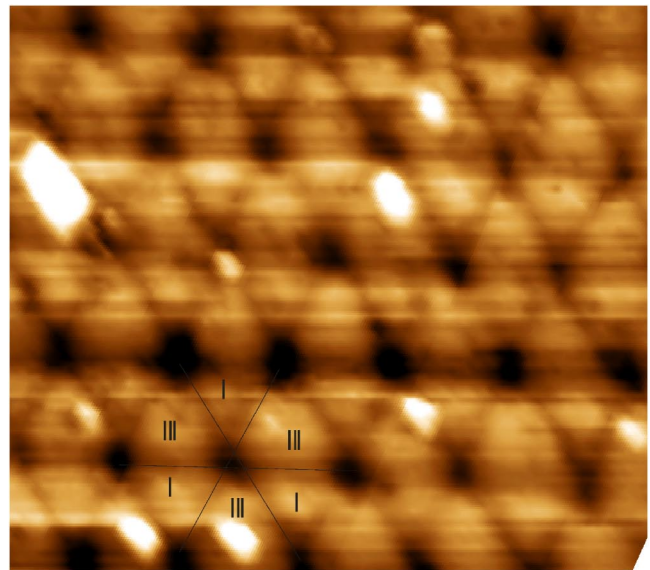


FIG. 2. ($600 \text{ \AA} \times 600 \text{ \AA}$) STM image of an ordered array of Fe islands formed on the superstructured magnetite surface (terrace (A)). Fe islands (white blobs) of 1 monolayer thickness are nucleated in the areas III of superstructure (Fig. 1). Inset shows enhanced contrast image. The terrace (B) contains randomly nucleated Fe islands nucleated.

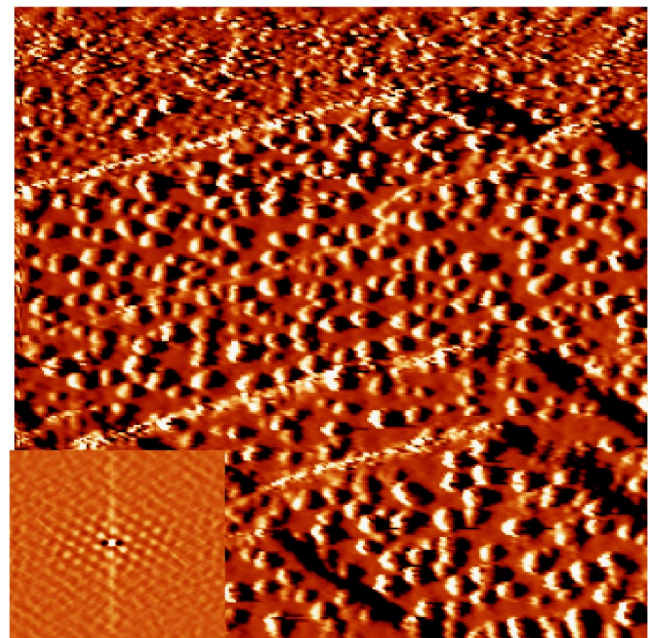
(111), which reconstructs under intrinsic stress to create a long-range order. It should be noted here that the topographical features (the corrugation and even the shape of the different areas) seen in Fig. 1 are very sensitive to the scanning conditions (tunneling bias, current, and tip properties) and originate from an electronic effect rather than representing the real geometry of the superstructure. The image in Fig. 1 can be interpreted as an image of a closed-packed oxygen lattice with local variations in the interatomic spacing according to the surface strain pattern,¹⁰ with Area I under tensile and the Area III under compressive stress.

The superstructure is stable at room temperature and is not significantly affected by adsorbates even after a few days in an UHV. These characteristics make it a very suitable template for the growth of self-assembled nanostructures. We have evaporated Fe films of 0.5 \AA and 0.2 \AA and 1 \AA thickness by electron-beam evaporation at room temperature and at a pressure of 3×10^{-10} Torr. Fe films were evaporated at a deposition rate of $0.5 \text{ \AA}/\text{min}$. The film thickness and the deposition rate were measured by a quartz crystal balance. LEED measurements carried out after the deposition confirmed the presence of a 42 \AA superlattice.

Figure 2 shows a STM image of the Fe nanoclusters nucleated in ordered fashion on top of the superstructure, which is still clearly visible. The thickness of the nanoclusters was measured to be $2.2 \pm 0.3 \text{ \AA}$. By using molecular simulation for the growth of Fe on the oxygen-terminated $\text{Fe}_3\text{O}_4(111)$ surface, we have established that Fe films grow preferentially along the (110) Fe-bulk plane. The Fe (110) in-plane interatomic periodicity is 2.48 \AA and the interlayer separation 2.03 \AA . We therefore conclude that the Fe islands



(a)



(b)

FIG. 3. (a) ($250 \text{ \AA} \times 220 \text{ \AA}$) STM image of 0.2 \AA Fe film deposited on superstructured magnetite surface. Fe islands start to nucleate on the area III. (b) ($1000 \text{ \AA} \times 1000 \text{ \AA}$) differential contrast STM image of 1 \AA Fe film deposited at the same substrate as in (a). Calculated self-correlation in the inset shows a relatively high degree order of 42 \AA periodicity.

represent 1 monolayer (ML) of iron. It is worth noting that the underlying superstructure is stable and is not affected by the deposition of the Fe film, and that the array of nanoclusters is stable at room temperature. Two terraces, A and B in Fig. 2, separated by a step height of $2.5 \pm 0.4 \text{ \AA}$ both correspond to oxygen termination. Terrace A is reconstructed, while B contains a number of surface defects, which inhibit the superstructure formation. More detailed data about magnetite (111) terminations can be found in Ref. 10. The Fe nanoclusters form a regular array on Terrace A only, while

Terrace **B** contains only randomly nucleated Fe islands. Terraces with no superstructure also exhibit a Fe decoration of the terrace edges, indicating that a higher diffusion rate on those terraces allows an Fe adatom to diffuse toward areas of higher surface energy.

It is clear from the STM image in Fig. 2 that the Fe islands nucleate preferentially on particular areas of the superstructure, creating an ordered array with the same periodicity as the superstructure. Further analysis of the STM images of lower coverage of iron [Fig. 3(a)] indicates that the nucleation is more likely to start on Area III of the superstructure. To study growth kinetic, we deposited 1 Å (0.6 ML) Fe film on the same substrate. The results presented in Fig. 3(b) suggest, that after Fe adatoms filled Area III, they start to form a second layer on top of each cluster. This means a switch of the Fe cluster growth to three-dimensional (3D) mode at coverage well below the completion of a closed monolayer.

III. DISCUSSION AND CONCLUSIONS

Despite the fact that Fe—O bonds are much stronger than Fe—Fe, it appears, the metal-metal interaction controls the growth even at submonolayer coverage. Weak reactive behavior of surface oxygen is considered in previous theoretical study¹¹ and 3D growth at submonolayer coverage is demonstrated in case of V and Fe grown on TiO₂.^{7,12} Goniakowski and Noguera in¹³ proposed that the two-dimensional (2D) growth of Pd on MgO is due to a significant electron transfer between the deposited metal and the oxygen at the surface, which significantly enhances the adhesion energy. A similar behavior could be expected for the deposition of Fe on the oxygen-terminated Fe₃O₄(111) surface.

To the best of our knowledge, well defined arrays of metal nanostructures were successfully grown on reconstructed

metal oxides in only two cases. In one case, Pd grown on an alumina film exhibits a self-ordering behavior, forming an array of nanoclusters with a period equal to that of the surface superstructure.⁹ In the second case, the FeO film used in Shaikhutdinov's *et al.*⁸ experiment as a substrate possesses a long-range order, which is attributed to the lattice mismatch between the FeO film and Pt (111) substrate. Although the authors did not claim that the growth takes place on preferential nucleation sites, the shape of the islands and the correlation between the superstructure periodicity and the island's size are a strong indication that this is the case. In both cases, the oxide thin film and substrate form a coincidence structure as a result of the lattice mismatch between them. Similar to our case, one of the characteristics of such structures is a long-range modulation of the surface strain, which is always responsible for local changes in the diffusion barrier.¹⁴ Although, a diffusion barrier increase in areas under tensile stress has been observed for growth on metal substrates,^{15–17} which is contrary to our observation. However, the long-range surface strain modulation observed in our case leads to a difference in coordination between the top layer and the underlying layers (bulk) in Areas I and III. Since the stacking sequence is known to affect the adsorption properties,¹⁸ we propose this as an explanation for the formation of the preferential nucleation sites as opposed to a mere alteration of the diffusion barrier and binding energy by a uniform strain.

To summarize, the results presented here can be divided in two parts. First, the patterned surface of magnetite (111) presents preferential nucleation sites for the formation of Fe nanoclusters. Second, the reported Fe growth on the superstructured magnetite surface switches from 2D to 3D mode at coverage well below a complete monolayer, which makes it potentially suitable for the formation of a 3D nanocluster array.

¹G. Karczewski, S. Mackowski, M. Kutrowski, T. Wojtowicz, and J. Kossut, *Appl. Phys. Lett.* **74**, 3011 (1999).

²I. L. Aleiner and V. I. Fal'ko, *Phys. Rev. Lett.* **87** 256801(2001).

³M. Bayer, A. Kuther, A. Forchel, A. Gorbunov, V. B. Timofeev, F. Schafer, J. P. Reitmaier, T. L. Reinecke, and S. N. Walck, *Phys. Rev. Lett.* **82**, 1748 (1999).

⁴S. Mitani, S. Takahashi, K. Takanashi, K. Yakushiji, S. Maekawa, and H. Fujimori, *Phys. Rev. Lett.* **81**, 2799 (1998).

⁵Y. Peng, H. L. Zhang, S. L. Pan, and H. L. Li, *J. Appl. Phys.* **87**, 7405 (2000);.

⁶M. Baumer and H.-J. Freund, *Prog. Surf. Sci.* **61**, 127 (1999).

⁷U. Diebold, *Surf. Sci. Rep.* **48**, 53 (2003); L. Zhang, R. Persaud, and T. E. Madey, *Phys. Rev. B* **56**, 10549 (1997).

⁸S. K. Shaikhutdinov, R. Meyer, D. Lahav, M. Baumer, T. Kluner, and H.-J. Freund, *Phys. Rev. Lett.* **91**, 076102 (2003).

⁹S. Degen, C. Becker, and K. Wandelt, *Faraday Discuss.* **125**, 343 (2004).

¹⁰N. Berdunov, S. Murphy, G. Mariotto, and I. V. Shvets, *Phys.*

Rev. B **70**, 085404 (2004).

¹¹K. M. Neyman, C. Inntam, V. A. Nasluzov, R. Kosarev, and N. Rosch, *Appl. Phys. A: Mater. Sci. Process.* **78**, 823 (2004).

¹²J. Biener, M. Baumer, J. Wang, and R. J. Madix, *Surf. Sci.* **450**, 12 (2000).

¹³J. Goniakowski, and C. Noguera, *Phys. Rev. B* **66**, 085417 (2002).

¹⁴M. I. Larsson, R. F. Sabiryanov, K. Cho, and B. M. Clemens, *Surf. Sci. Lett.* **536**, L389 (2003).

¹⁵H. Brune, K. Bromann, H. Röder, K. Kern, J. Jacobsen, P. Stoltze, K. Jacobsen, and J. Nørskov, *Phys. Rev. B* **52**, 14380 (1995).

¹⁶C. Ratsch, A. P. Seitsonen, and M. Scheffler, *Phys. Rev. B* **55**, 6750 (1997).

¹⁷I. V. Shvets, and S. Murphy *et al.* (unpublished); also cond-mat/0405148.

¹⁸H. Brune, M. Giovannini, K. Bromann, and K. Kern, *Nature (London)* **394**, 451 (1998).